ZIBELINE INTERNATIONAL™ PUBLISHING

ISSN: 2521-0858 (Print)
ISSN: 2521-0866 (Online)
CODEN: SHJCAS

Science Heritage Journal (GWS)

DOI: http://doi.org/10.26480/gws.01.2026.01.08

RESEARCH ARTICLE

INVESTIGATING THE MAGNETIC PROPERTIES OF ZIG-ZAG SINGLE-WALLED (8,0) CARBON NANOTUBE WITH NIKIFOROV-UVAROV (NU) METHOD.

Ikechukwu Otete

Department of Physics, Faculty of Science Federal University, Otuoke, Nigeria
****Corresponding Author Email: oteteike@yahoo.com***

ARTICLE DETAILS

Article History:

Received 23 October 2025
Revised 08 November 2025
Accepted 24 December 2025
Available online 04 February 2026

ABSTRACT

An investigation into the magnetic properties of zig-zag single-walled (8,0) carbon nanotube is done. The Nikiforov-Uvarov method (NU) is used to solve the Schrödinger wave equation containing the quantum Hamiltonian of a charged particle confined in Deng-Fan Hulthen potential in the presence of applied external fields in perpendicular direction. The energy eigen value equation and the wave function are obtained. The partition function is calculated from the energy equation obtained. With the partition function, the magnetic properties; magnetization and susceptibility as a function of temperature, tube's diameter and Aharonov-Bohm flux are evaluated. The results of the analysis showed that the zig-zag single-walled (8,0) carbon nanotube has a negative magnetic susceptibility.

KEYWORDS

Magnetization, Magnetic Susceptibility, Magnetic Properties and Zig-Zag Singled-Walled (8,0) Carbon Nanotube.

1. INTRODUCTION

According to the discovery of carbon nanotubes (CNTs) and fullerenes with the attendant theoretical research on their properties have made their importance prominent in nanotechnology (Michael, 2006). CNTs are seen as one of the strongest materials with very high elasticity, high conductivity, miniature in size with good stability and their robust nature allow them to withstand chemically hostile environments. This miniature nature and their high surface area make them suitable candidates for the attachment and assembly of nanoparticles (NPs) on their surface. Their electrical, magnetic and even their physical properties can be improved significantly when either their internal cavity or external surface are decorated with different inorganic NPs using various experimental procedures (Ado and Mildred, 2008 ; Kim and Rina, 2011).

CNTs are sheets of graphene rolled around a central axis, forming hollow cylindrical shapes. CNTs are in two types-single-walled carbon nanotubes (SWCNT) and Multi-walled carbon nanotube (MWCNT). CNTs comprises of network of carbon atoms in hexagonal form. Their diameter is in the neighborhood of 1 and 2 nanometers while their length could be several micrometers (Hossein, 2020). Due to the small nanoscale diameter, the confinement and movement of electrons is along their length, hence, CNTs are regarded as one dimensional (1D) nanomaterials (Philip and Deji, 2011).

The SWCNTs are rolled-up cylindrical sheets of graphene made up of benzene type hexagonal network of carbon atoms that are sp^2hybridized (Saifuddin, 2013 ; Sebastien, 2013). Their diameter is in the range of 1 to 2 nanometer with lengths of several micrometer to centimeters. They can be metallic or semiconductor based on their stacking or arrangement of the carbon atoms/ the arrangement of their helicity (Phaedon, 2003 ; Ando, 2005). MWCNTs are made up of layers of graphene sheets rolled-up to form a concentric tubular shape. They can be regarded as arrays of concentric SWCNTs stacked in between each other with a spacing of about 0.34 nanometer (Saifuddin, 2013).

1.1 Magnetic Properties of Carbon nanotubes

Carbon nanotubes in their pure forms are non-magnetic. Although CNT is diamagnetic in nature but it can become magnetized when magnetic field is applied in a direction of 180° to it (Rees, 2021). Also, the tube chirality, Fermi energy level and the magnetic field direction with respect to the tube axis can determine either the paramagnetic and diamagnetic behavior of single-walled carbon nanotubes (SWCNTs) (Keun, 2008). According to the study, CNTs show considerable large diamagnetic and paramagnetic behaviors in the presence of weak magnetic field based on the direction of the field, Fermi energy and geometric parameters like helicity and tube radius (Jian, 1995). Carbon nanotubes (SWCNTs) demonstrate considerable features of diamagnetism when magnetic field is applied perpendicular to the axis (Oleg, et al, 2020). The diamagnetism of CNTs is anisotropic in nature and it has a correlation to an Aharonov-Bohm (AB) effect. However, catalyst like Fe, Ni or Co can bring about paramagnetism in CNTs (Ibwanga et al, 2021). Therefore, the synthesis of magnetic carbon nanotubes (MCNTs) will open up new vista of applications in nano biotechnology and biomedical fields. MCNTs can be produced via various means. Some of these methods include filling process, sol-gel process, chemical vapor deposition (CVD), self-assembly, template-based synthesis, hydrothermal/solvothermal and pyrolysis procedure detonation induced reaction (Mehrdad et al, 2017). Possible usage of magnetic CNTs is in the area of information technology. Here, a special hybrid of magnetic CNTs containing single-molecule magnets embedded in non-magnetic CNTs are synthesized. These synthesized material possess both magnetic and functional properties of nanotubes which can be potentially used in designing magnetic data storage and information processing devices (Chen and Valery, 2024). The magnetic properties of CNTs is poor naturally, and of course could limit their wide range of application in electromagnetic wave absorbers (use as radars-absorbent materials), magnetic sensors, and magnetic stability system amongst others. However, their magnetic properties can be improved

Quick Response Code	Access this article online	
	Website: www.jscienceheritage.com	**DOI:** 10.26480/gws.01.2026.01.08

Cite The Article: Ikechukwu Otete (2026). Investigating The Magnetic Properties of Zig-Zag Single-Walled (8,0) Carbon Nanotube with Nikiforov-Uvarov (Nu) Method. Science Heritage Journal, 10(1): 01-08.

upon if magnetic nanoparticles are in the design of nanotubes. A deluge of experimental studies, molecular dynamics simulations and first-principle methods have been done on CNTs using some empirical potentials like Tersoff, Brenner, Morse and Lennard Jones, to investigate the various properties of CNTs but not with NU method. Therefore, being fascinated by the versatility in usage of the magnetic properties of CNTs which have not been studied theoretically within the frame work of Deng-Fan-Hulthen potential in applied magnetic field and AB flux field with NU method, investigating the magnetic properties of CNTs is worthwhile.

The Aharonov-Bohm (AB) phase created around cylindrical nanotube in a magnetic field parallel to its axis alters the band structure. However, their metallicity can be controlled by the application of external magnetic fields (Abbasi, 2024). A metallic CNT can be transformed into a semiconducting CNT and semiconducting tube can become metallic due to the effect of applied magnetic field. Also, Zeeman splitting, the magnitude and the orientation of the magnetic field are key factors that determine the metallicity transitions of carbon nanotubes in the presence of magnetic flux (Tsai, 2005). This situation results in unusual behavior of magneto-resistance (Ado and Mildred, 2008 ; Ovchinnikov et al, 1998).

Diamagnetic material shows negative magnetic susceptibility. The negative values of the susceptibility implies that diamagnetic materials becomes magnetized when in an area of applied magnetic field. This magnetization points opposite to the applied field. The susceptibility of this diamagnetic materials has nearly a constant values independent of temperature. However, in a perpendicular magnetic field, metallic and semiconducting SWCNTs exhibit diamagnetism. Meanwhile the magnetic susceptibility anisotropy of semiconducting SWCNTs are lesser in values compare to metallic SWCNTs (Searles et al, 2010). Zig-zag single-walled (8,0) carbon nanotube possesses a length of 6.403(Å) with symmetry group, P4/mmm (Constantinos et al, 2019). At the Fermi energy, the density of state is zero showing that it is a semiconductor. The calculated band gap is 1.360eV while the simulated band gap is 1.4078eV. The total number of unit cells and carbon atoms in the overall unit cells are16 and 32 respectively. In its molecular structure, the total number of unit cells, carbon atoms and hexagons are 208, 416 and 192 (Devi and Rakesh, 2017 ; Devi et al, 2012).

In this work, the Nikiforov-Uvarov (NU) method will be used to solve the Schrödinger wave equation containing the Hamiltonian of a charged particle with the Deng-Fan-Hulthen Potential (DFHP) in the presence of applied magnetic field and Aharonov-Bohm (AB) flux in perpendicular direction to obtain the energy eigen value equation and wave function. Thereafter, the partition function for the zig-zag single-walled (8,0) carbon nanotube (SWCNT) will be calculated. With the partition function, the magnetic properties of the nanotube will be investigated.

This paper is organized as follows; in section two, the NU method will be used to solve the Schrödinger wave equation containing the Hamiltonian of a charged particle to obtain the energy equation and wave function. The partition function is calculated in section three with the graphical plots while section four will be results and discussion. The last section will be conclusion followed by references.

2. Theoretical Model And Methodology

For a charged particle, the quantum Hamiltonian with the Schrödinger equation placed in a region of Deng-Fan-Hulthen potential interacting in an external magnetic field B and Ahanorov-Bohm (AB) flux in a co-ordinate system that is cylindrical is written as:

$$\frac{1}{2\mu}(i\hbar\vec{\nabla}- qc^{-1}\vec{A})^2+ D_e\left(1-\frac{\mathrm{V}}{(e^{\theta r}-1)}\right)^2-\frac{V_o e^{\theta r}}{(1- e^{-\theta r})}=E_{(n,m)}\psi_{(\rho,\varphi,z)} \quad (1)$$

where $\mathrm{V}=e^{\theta r_e}$ -1, D_e stands for dissociation energy, r_e represents molecular bond length, r is the inter-nuclear distance, θ, the range of the potential well and V_o is the potential strength (Otete et al, 2024).

Here, μ is taken to be the effective mass for the CNT. The summation of two terms gives the vector potential $\vec{A}$, written as $\vec{A}=\vec{A}_1+\vec{A}_2$ and our Coulomb gauge is written as $\nabla\times\vec{A}_1=\vec{B}$ and $\nabla\times\vec{A}_2=0$ where B_z stands for the applied magnetic field along the z-axis. The additional magnetic flux Φ_{AB} is as a result of the solenoid. Therefore, the vector potential in the cylindrical coordinate system, has the azimuthal components written as (Otete et al, 2024):

$$\vec{A}_1=\frac{\vec{B}e^{-\theta r}}{(1-e^{-\theta r})},\vec{A}_2=\frac{\Phi_{AB}}{2\pi r}\widehat{\Phi}\ \text{So},\ \vec{A}=\left(0,\frac{\vec{B}e^{-\theta r}}{(1-e^{-\theta r})}+\frac{\Phi_{AB}}{2\pi r},0\right) \quad (2)$$

The Deng-Fan-Hulthen Potential which is the confining potential. It is of two potentials-Deng-Fan and Hulthen potentials.

The wave function in the cylindrical coordinates is written as:

$$\psi_{(r,\varphi)}=\frac{1}{\sqrt{2\pi}}e^{im\varphi}\ U_{nm,}(r)\ m=0,\pm1,\pm2\ldots \quad (3)$$

where m stands for the magnetic quantum number. When the confining potential, vector potential and the wave function are inserted into Eq. (1), a second-order differential equation of Eq. (4) is obtained:

$$\frac{d^2U_{nm}(r)}{dr^2}+\frac{2\mu}{\hbar^2}[E-D_e(1-\frac{\mathrm{V}}{(e^{\theta r}-1)})^2+\frac{V_o e^{-\theta r}}{(1-e^{-\theta r})}-\frac{2\hbar me\theta\vec{B}e^{-\theta r}}{c(1-e^{-\theta r})}-\frac{e^2\vec{B}e^{-2\theta r}}{c^2(1-e^{-\theta r})^2}-\frac{e^2\vec{B}\Phi_{AB}e^{-\theta r}}{c^2(1-e^{-\theta r})^2 2\pi r}-\frac{((m+\zeta)-\frac{1}{4})}{r^2}]U_{nm}(r)=0 \quad (4)$$

The Greene and Aldrich improved approximation scheme given in the Eq. (5), will help to solve the differential equation of Eq. (4) that has both exponential and radial terms (Otete et al, 2024).

$$\frac{1}{r^2}\approx\theta^2[d_o+\frac{e^{-\theta r}}{(1-e^{-\theta r})^2}] \quad (5)$$

By inserting Eq. (5) into Eq. (4) we have

$$\frac{d^2U_{nm}(r)}{dr^2}+[\frac{2\mu E}{\hbar^2}-\frac{2\mu D_e}{\hbar^2}+\frac{4\mu D_e\mathrm{V}e^{-\theta r}}{\hbar^2(1-e^{-\theta r})}\frac{2D_e\mathrm{V}^2e^{-2\theta r}}{\hbar^2(1-e^{-\theta r})^2}+\frac{2V_o e^{-\theta r}}{\hbar^2(1-e^{-\theta r})}-\frac{2m\eta\theta\vec{B}e^{-\theta r}}{\hbar^2(1-e^{-\theta r})^2}-\frac{\eta^2\vec{B^2}e^{-2\theta r}}{\hbar^2(1-e^{-\theta r})^2}-\frac{\eta^2\theta\vec{B}\Phi_{AB}e^{-\theta r}}{\hbar^2(1-e^{-\theta r})^2\pi}-((m+\zeta)-\frac{1}{4})\theta^2(d_o+\frac{e^{-\theta r}}{(1-e^{-\theta r})^2})]U_{nm}(r) \quad (6)$$

Where $\eta=\frac{e}{c},\Phi_o=\frac{\hbar c}{e},\zeta=\frac{\Phi_{AB}}{\Phi_o}$ and $\mathrm{V}=e^{\theta r}-1$, c is the speed of light.

Using the transformation $\mathcal{S}=e^{-\theta r}$ (7)

After differentiating twice, you will obtain:

$$\frac{d^2}{d\mathcal{S}^2}=\frac{\theta^2\mathcal{S}^2d^2}{d\mathcal{S}^2}+\frac{\theta^2\mathcal{S}d}{d\mathcal{S}} \quad (8)$$

Substituting Eq. (8) into Eq. (6) and divide through by $\theta^2\mathcal{S}^2$ the result will be:

$$\frac{d^2U_{nm}}{d\mathcal{S}^2}+\frac{1}{\mathcal{S}}\frac{dU_{nm}}{d\mathcal{S}}+\frac{1}{\mathcal{S}^2}\left[\frac{2\mu E}{\hbar^2\theta^2}-\frac{2\mu D_e}{\hbar^2\theta^2}+\frac{4\mu D_e\mathrm{V}\mathcal{S}}{\hbar^2\theta^2(1-\mathcal{S})}-\frac{2\mu D_e\mathrm{V}^2\mathcal{S}^2}{\hbar^2\theta^2(1-\mathcal{S})^2}+\frac{2\mu V_o\mathcal{S}}{\hbar^2\theta^2(1-\mathcal{S})}-\frac{2m\eta\vec{B}\mathcal{S}}{\hbar\theta(1-\mathcal{S})^2}-\frac{\eta^2\vec{B}^2\mathcal{S}^2}{\hbar^2(1-\mathcal{S})^2},,-\frac{\eta^2\vec{B}\Phi_{AB}\mathcal{S}}{\hbar^2\theta(1-\mathcal{S})^2\pi}-\left((m+\zeta)^2-\frac{1}{4}\right)\left(d_o+\frac{\mathcal{S}}{(1-\mathcal{S})^2}\right)\right]U_{nm}(r)=0 \quad (9)$$

We use the following dimensionless symbols for mathematical convenience

$$-\varepsilon=\frac{2\mu(E_{nm}-D_e)}{\hbar^2\theta^2}\ ,\ \chi_1=\frac{4\mu D_e\mathrm{V}}{\hbar^2\theta^2}\ ,\ \chi_2=\frac{2\mu D_e\mathrm{V}^2}{\hbar^2\theta^2}\ ,\ \mathfrak{B}=\frac{2\mu V_o}{\hbar^2\theta^2}\ ,\ \mathfrak{b}=\frac{2m\eta\vec{B}}{\hbar\theta},\gamma_1=\frac{\eta^2\vec{B}^2}{\hbar^2\theta^2},\gamma_2=\frac{\eta^2\vec{B}\Phi_{AB}}{\hbar^2\theta^2\pi},V=\left((m+\zeta)^2-\frac{1}{4}\right) \quad (10)$$

Equation (9) can be rewritten with respect to these dimensionless symbols as:

$$\frac{d^2U_{nm}}{d\mathcal{S}^2}+\frac{(1-\mathcal{S})}{\mathcal{S}(1-\mathcal{S})}\frac{dU_{nm}}{d\mathcal{S}}+\frac{1}{\mathcal{S}^2(1-\mathcal{S})^2}[-\varepsilon(1-\mathcal{S})^2+\chi_1(1-\mathcal{S})\mathcal{S}-\chi_2(\mathcal{S}^2)+\mathfrak{B}(1-\mathcal{S})\mathcal{S}-\mathfrak{b}(\mathcal{S})-\gamma_1(\mathcal{S}^2)-\gamma_2(1-\mathcal{S})\mathcal{S}-Vd_o(1-\mathcal{S})^2-V(\mathcal{S})]U_{nm}=0 \quad (11)$$

Subsequently, Eq. (11) can be evaluated further as:

$$\frac{d^2U_{nm}}{d\mathcal{S}^2}+\frac{(1-\mathcal{S})}{\mathcal{S}(1-\mathcal{S})}\frac{dU_{nm}}{d\mathcal{S}}+\frac{1}{\mathcal{S}^2(1-\mathcal{S})^2}[-(\varepsilon+\chi_1+\chi_1+\mathfrak{B}+\gamma_1-\gamma_2+Vd_o)\mathcal{S}^2+(2\varepsilon+\chi_1+\mathfrak{B}-\mathfrak{b}-\gamma_2+2Vd_o-V)\mathcal{S}-(\varepsilon+Vd_o)]U_{nm}(r)=0 \quad (12)$$

Eq. (12) is compared with the parametric form of the NU of Eq. (13) is written (Otete and Eleje, 2023) as:

$$U^{"}+\frac{\theta_1-\theta_2\mathcal{S}}{\mathcal{S}(1-\theta_3\mathcal{S})}U'+\left[\frac{-\xi_1\mathcal{S}^2+\xi_2\mathcal{S}-\xi_3}{\mathcal{S}^2(1-\theta_3\mathcal{S})^2}\right]U_{(\mathcal{S})}=0 \quad (13)$$

The energy eigen values equation according to the NU is written as

$$\theta_2 n-(2n+1)\theta_5+(2n+1)[\sqrt{\theta_9}+\theta_3\sqrt{\theta_8}]+n(n-1)\theta_3+\theta_7+2\theta_3\theta_8+2\sqrt{\theta_8\theta_9}=0 \quad (14)$$

The corresponding wave function is given as:

$$U_{nm}(\mathcal{S})=\mathcal{S}^{\theta_{12}}(1-\theta_3\mathcal{S})^{-\theta_{12}-\theta_{13}/\theta_3}p_n^{\theta_{10-1},(\frac{\theta_{11}}{\theta_3})-(\theta_{10}-1)}(1-2\theta_3\mathcal{S}) \quad (15)$$

where the following parameters are written as

$$\theta_4=\frac{1}{2}(1-\theta_1) \quad (16)$$

$$\theta_5=\frac{1}{2}(\theta_2-2\theta_3) \quad (17)$$

$$\theta_6=\theta_5+\xi_1 \quad (18)$$

$$\mathcal{B}_7 = 2\mathcal{B}_4\mathcal{B}_5 - \xi_2 \quad (19)$$

$$\mathcal{B}_8 = \mathcal{B}^2{}_4 + \xi_3 \quad (20)$$

$$\mathcal{B}_9 = \mathcal{B}_3(\mathcal{B}_7 + \mathcal{B}_3\mathcal{B}_8) + \mathcal{B}_6 \quad (21)$$

$$\mathcal{B}_{10} = \mathcal{B}_1 + 2\mathcal{B}_4 + 2\sqrt{\mathcal{B}_8} \quad (22)$$

$$\mathcal{B}_{11} = \mathcal{B}_2 - 2\mathcal{B}_5 + 2(\sqrt{\mathcal{B}_9} + \mathcal{B}_3\sqrt{\mathcal{B}_8}) \quad (23)$$

$$\mathcal{B}_{12} = \mathcal{B}_4 + \sqrt{\mathcal{B}_8} \quad (24)$$

$$\mathcal{B}_{13} = \mathcal{B}_5 - (\sqrt{\mathcal{B}_9} + \mathcal{B}_3\sqrt{\mathcal{B}_8}) \quad (25)$$

When Eq. (12) is compared with the parametric form of the NU of Eq. (13) the following, parameters can be found:

$$\mathcal{B}_1 = \mathcal{B}_2 = \mathcal{B}_3 = 1 \quad (26)$$

$$\xi_1 = \varepsilon + \chi_1 + \chi_1 + \mathcal{B} + \gamma_1 - \gamma_2 + Vd_o \quad (27)$$

$$\xi_2 = 2\varepsilon + \chi_1 + \mathcal{B} - \mathcal{B} - \Lambda_2 + 2Vd_o - V \quad (28)$$

$$\xi_3 = \varepsilon + Vd_o \quad (29)$$

From Eqs. (16-21) we obtain

$$\mathcal{B}_4 = \frac{1}{2}(1 - \mathcal{B}_1) = 0,\ \mathcal{B}_5 = \frac{1}{2}(\mathcal{B}_2 - 2\mathcal{B}_3) = -\frac{1}{2},\quad \mathcal{B}_6 = \mathcal{B}_5^2 + \xi_1 = \frac{1}{4} + \varepsilon + \chi_1 + \chi_1 + \mathcal{B} + \gamma_1 - \gamma_2 + Vd_o \quad (30)$$

$$\mathcal{B}_7 = 2\mathcal{B}_4\mathcal{B}_5 - \xi_2 = -(2\varepsilon + \chi_1 + \mathcal{B} - \mathcal{B} - \gamma_2 + 2Vd_o - V) \quad (31)$$

$$\mathcal{B}_8 = \mathcal{B}_4^2 + \xi_3 = \varepsilon + Vd_o \quad (32)$$

$$\mathcal{B}_9 = \mathcal{B}_3\mathcal{B}_7 + \mathcal{B}_3^2\mathcal{B}_8 + \mathcal{B}_6 = \frac{1}{4} + \mathcal{B} + V + \gamma_1 + \chi_2 \quad (33)$$

Recall that in Eq.(10) , $-\varepsilon = \frac{2\mu(E_{nm} - D_e)}{\hbar^2\mathcal{B}^2}$ (34)

So, substituting Eqs. (30-33) into Eq. (14) and carrying out some algebra the energy eigenvalue equation of the Deng-Fan-Hulthen potential is obtained as:

$$E_{nm} = -\frac{\hbar^2\mathcal{B}^2}{2\mu}\left[\left(\frac{(\rho - \Lambda)}{2(\tau + \sqrt{\rho})} - \frac{(\tau + \sqrt{\rho})}{2}\right)^2 - Vd_o + D_e\right] \quad (35)$$

where

$$\rho = \frac{1}{4} + \mathcal{B} + V + \gamma_1 + \chi_2,\ \Lambda = -\chi_1 - \mathcal{B} + \mathcal{B} + \gamma_2 + V, \tau = n + \frac{1}{2} \quad (36)$$

Using the dimensionless symbols of Eq. (10), Eq. (36) can be re-written as:

$$\rho = \frac{1}{4} + \frac{2m\eta\vec{B}}{\hbar\mathcal{B}} + (m + \zeta)^2 - \frac{1}{4} + \frac{\eta^2\vec{B}^2}{\hbar^2\mathcal{B}^2} + \frac{2\mu D_e V^2}{\hbar^2\mathcal{B}^2} \quad (37)$$

$$\Lambda = -\frac{4\mu D_e V}{\hbar^2\mathcal{B}^2} - \frac{2\mu V_o}{\hbar^2\mathcal{B}^2} + \frac{2m\eta\vec{B}}{\hbar\mathcal{B}} + \frac{\eta^2\vec{B}\Phi_{AB}}{\hbar^2\mathcal{B}\pi} + (m + \zeta)^2 - \frac{1}{4} \quad (38)$$

From Eqs. (22-25) we determine

$$\mathcal{B}_{10} = \mathcal{B}_1 + 2\mathcal{B}_4 + 2\sqrt{\mathcal{B}_8} = 1 + 2\sqrt{\varepsilon + Vd_0} \quad (39)$$

$$\mathcal{B}_{11} = \mathcal{B}_2 - 2\mathcal{B}_5 + 2((\mathcal{B}_9 + \mathcal{B}_3\mathcal{B}_8)^{1/2}) = 2 + 2\left(\sqrt{\frac{1}{4} + \mathcal{B} + V + \gamma_1 + \chi_2 + \varepsilon + Vd_0}\right) \quad (40)$$

$$\mathcal{B}_{12} = \mathcal{B}_4 + \sqrt{\mathcal{B}_8} = \sqrt{\varepsilon + Vd_0} \quad (41)$$

$$\mathcal{B}_{13} = \mathcal{B}_5 - ((\mathcal{B}_9)^{1/2} + \mathcal{B}_3(\mathcal{B}_8)^{1/2}) = -\frac{1}{2} - \left(\sqrt{\frac{1}{4} + \mathcal{B} + V + \gamma_1 + \chi_2} + \sqrt{\varepsilon + Vd_0}\right) \quad (42)$$

Substituting Eqs. (39-42) into Eq. (15) the wave function written in Eq. (43) is obtained.

$$U_{nm}(\mathcal{S}) = \mathcal{S}^{\sqrt{\varepsilon + Vd_0}}(1 - \mathcal{S})^{\frac{1}{2} + \sqrt{\frac{1}{4} + \mathcal{B} + V + \gamma_1 + \chi_2}} P_n^{2\sqrt{\varepsilon + Vd_0},\, 2\sqrt{\frac{1}{4} + \mathcal{B} + V + \gamma_1 + \chi_2}}(1 - 2\mathcal{S}) \quad (43)$$

3. THE PARTITION FUNCTION

The partition function known as the distribution function that depends on temperature (Ikot et al, 2018). It is referred to as the number of times larger the total number of particles is than the number of particles in the ground state. If N represents the total number of particles and n_o represents the number of particles in the lowest or ground state energy.

Then,

$$\frac{N}{n_o} = \text{Partition function}, Z \quad (44)$$

The size of the partition function is dependent on both the energy of the excited state and temperature of the system. The energies partitioned or distributed over the different energy levels is known through the partition function. It is dependent on the temperature, T through beta, β. For all possible states a particle can assume, we defined the partition function as the summation of $e^{-\epsilon_i}/kT$ over it (Chang and John, 1985).

The partition function is important because once the partition function is known, the thermodynamic quantities or functions, heat capacities, entropies and equilibrium constant can be calculated from it (Atkins and Paula, 2009).

With the knowledge of the partition function, the information of the eigen values embedded in the thermodynamic quantities can be extracted.

We write the partition function as:

$$Z(\beta) = \sum_n^{v_{max}} e^{-\beta E_{nm}} \quad (45)$$

Where $\beta = (KT)^{-1}$ with K as the Boltsmann constant and T the temperature (Zhou and Dai 2018). E_{nm} is the energy of the nth bound state where $n = 0, 1, 2, 3 \ldots, v_{max}$.

$$E_{nm} = -\hbar^2\vartheta^2\left(\frac{G_1 - (n+\rho)^2}{2(n+\rho)}\right)^2 + G_2 \quad (46)$$

where

$$G_1 = \frac{1}{4} + \frac{2m\eta\vec{B}}{\hbar\mathcal{B}} + (m + \zeta)^2 - \frac{1}{4} + \frac{\eta^2\vec{B}^2}{\hbar^2\mathcal{B}^2} + \frac{2\mu D_e V^2}{\hbar^2\mathcal{B}^2} + \frac{4\mu D_e}{\hbar^2\mathcal{B}^2} - \frac{2\mu V_o}{\hbar^2\mathcal{B}^2} + \frac{2m\eta\vec{B}}{\hbar\mathcal{B}} + \frac{\eta^2\vec{B}\Phi_{AB}}{\hbar^2\mathcal{B}\pi} + (m + \zeta)^2 - \frac{1}{4} \quad (47)$$

$$G_2 = \left((m + \zeta)^2 - \frac{1}{4}\right) d_o\left(\frac{\hbar^2\mathcal{B}^2}{2\mu}\right) + D_e \quad (48)$$

Therefore, equation (45) can be recast as:

$$Z(\beta) = \sum_n^{v_{max}} e^{-\beta\left[\frac{\hbar^2\mathcal{B}^2}{2\mu}\left(\frac{G_1 - (n+\rho)^2}{2(n+\rho)}\right)^2 + G_2\right]} \quad (49)$$

In the classical limit, the summation of equation (48) is replaced by an integral therefore we have

$$Z_{(\beta)} = \int_0^v e^{\left(Kl^2\beta + \frac{N\beta}{l^2} + P\beta\right)} dl, l = n + \rho \quad (50)$$

where

$$K = \frac{\hbar^2\vartheta^2}{8\mu}, N = -\frac{\hbar^2\vartheta^2 G_1^2}{8\mu}, P = -\left(\frac{\hbar^2\vartheta^2 G_1}{4\mu} + G_2\right) \quad (51)$$

In order to obtain the partition function of the system, the Maple software is employ to evaluate Eq. (50) as:

$$\frac{1}{2}e^{k.\beta.l^2 + P.\beta\sqrt{N.\beta}}\left(\frac{2.v.e^{\frac{N\beta}{v^2}}}{\sqrt{N.\beta}} - \frac{2\sqrt{N.\beta}\ \sqrt{\pi}\ erfi\left(\frac{N.\beta}{v}\right)}{\sqrt{N.\beta}} - 2\sqrt{\pi}\right) \quad (52)$$

When one has obtained the partition function as in Eqn. (52), the thermodynamic functions or quantities of the system which are the mean energy U, specific heat C_v, free energy$F$, entropy S, magnetic susceptibility χ, etc can be calculated from using the following relations [Khordad and Rastegar, 2017; Eshghi, and Mehraban, 2017):

$$\text{Mean energy } U = -\frac{\delta lnZ}{\delta\beta} \quad (53)$$

$$\text{Specific heat } C_v = \frac{\delta U}{\delta T} = K\beta^2\frac{\delta^2 lnZ}{\delta\beta^2} \quad (54)$$

Free energy $F = -KTlnZ$ (55)

Entropy $S = KlnZ - \frac{K\beta\delta lnZ}{\delta\beta}$ (56)

Thermal conductivity $K = \frac{1}{3}\rho c v^2 \tau$ (57)

Magnetization $M = -\frac{\partial F}{\partial B}$ (58)

Susceptibility $\chi = -\frac{\delta^2 F}{\delta B^2}$ (59)

Persistent current $I = -\frac{\partial F}{\partial \Phi}$ or $-\frac{e}{hc}\frac{\partial F}{\partial M}$ (60)

However, the focus on this work is on magnetization and magnetic susceptibility.

Magnetization of a material is a measure of how the energy of the system respond to a magnetic field. It is written as (David, 2012):

$$M = -\frac{\partial E}{\partial B} \quad (61)$$

Magnetization is in inverse proportion to the temperature in the limit of vanishing magnetic field. This $1/T$ phenomenon is referred to as Curie's Law (David, 2012).

After obtaining the magnetization M, when differentiated with respect to B, the temperature-dependent susceptibility will be obtained (Bahadir and Ashok, 2012). It can also be obtained when the free energy is differentiated twice (Ado and Mildred, 2008). From the thermodynamic perspective, magnetic susceptibility with the symbol χ_m refers to the degree of magnetization of a material in an applied magnetic field. It is regarded as the ratio of magnetization, $\vec{M}$ of sample or material to the applied external magnetic field strength H. Mathematically expressed (Cano et al, 2008) as:

Magnetic Susceptibility, $\chi = \lim_{|\Delta\vec{H}|\to 0} \frac{|\Delta\vec{M}|}{|\Delta\vec{H}|}$ (62)

As earlier stated, according to (Bahadir and Ashok, 2012), when Eq. (63) is differentiated twice, it will yield the magnetic susceptibility written down in Eq. (64).

Magnetization $M = -\frac{\partial F}{\partial B}$ (63)

Magnetic Susceptibility, $\chi = -\frac{\delta^2 F}{\delta B^2}$ (64)

With Maple software, the energy eigen values are obtained using Eq. (35) when the magnetic field and AB flux are switch off, that is kept at zero and when the magnetic field is at 4Tesla and the AB flux is kept at zero are tabulated in table 1. While table 2 is when the magnetic field is kept at zero and the AB flux are kept at values 2 and 4 respectively.

Table 1 : Energy eigen-values for zig-zag SWCNT (8,0) having magnetic field, $\vec{B}$ and AB flux, ζ with various n and m states

m	n	$\vec{B} = \zeta = 0$	$\vec{B} = 4T, \zeta = 0$
0	0	-3.587167552	-1.4822421212
0	1	-2.752342028	-1.3224113519
0	2	-2.521224573	-1.2728131617
0	3	-1.818120621	-1.1342030251
1	0	-3.480836113	-1.4256421283
1	1	-2.848705157	-1.3737658771
1	2	-2.318128155	-1.2358668143
1	3	-1.816740407	-1.1256547581
-1	0	-3.480836113	-1.4527353623
-1	1	-2.948705156	-1.3805171255
-1	2	-2.318128155	-1.2408847713
-1	3	-1.818740407	-1.1715186424
2	0	-3.476056441	-1.3743742114
2	1	-2.844305671	-1.2341251362
2	2	-2.314037811	-1.1235353547
2	3	-1.813401628	-1.0541567102
-2	0	-3.476056441	-1.2317181802
-2	1	-2.844305671	-1.1487212154
-2	2	-2.314037813	-1.0788347315
-2	3	-1.813201628	-1.0211306185

Table 2 : Energy eigen-values for zig-zag SWCNT (8,0) having magnetic field, $\vec{B}$ and AB flux, ζ with various n and m states

m	n	$\vec{B}=0,\zeta=2$	$\vec{B}=0,\zeta=4$
0	0	-0.4821945856	-0.4782520026
0	1	-0.3363621474	-0.3334493837
0	2	-0.2340272040	-0.2318032016
0	3	-0.2252116566	-0.2144865018
1	0	-0.1607586286	-0.1590160044
1	1	-0.1538465726	-0.1454205252
1	2	-0.1340052778	-0.1199438572
1	3	-0.1077537577	-0.1063601404
-1	0	-0.1022229082	-0.0954692749
-1	1	-0.0862996920	-0.0749723805
-1	2	-0.0617849647	-0.0470555549
-1	3	-0.2252116566	-0.0289648279
2	0	-0.1999940563	-0.1822018376
2	1	-0.1538465726	-0.1454205252
2	2	-0.1340052778	-0.1119943857
2	3	-0.1036294162	-0.0854792316
-2	0	-0.1022229082	-0.0954692749
-2	1	-0.0862996920	-0.0749723805
-2	2	-0.0617849647	-0.0470555549
-2	3	-0.0311052979	-0.0142438138

Here, in fig. 1 and 2 are the graphical plots of magnetization versus temperature and tube diameter. In fig.3, 4 and 5 are the graphical plots of magnetic susceptibility versus temperature, tube diameter and AB flux.

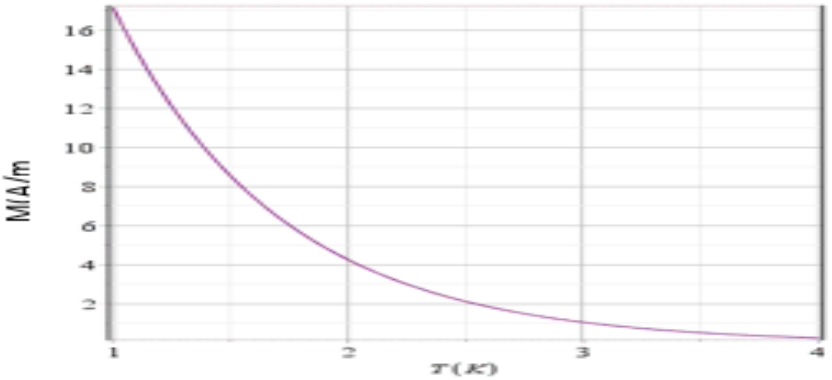

Figure 1: Plot of Magnetization versus Temperatures

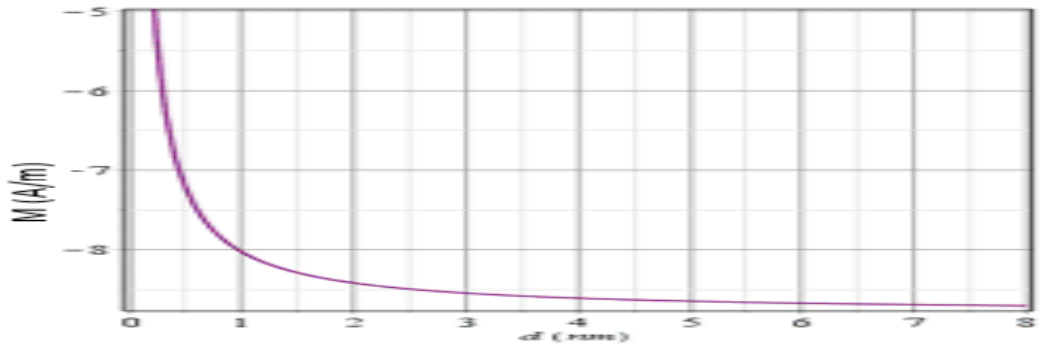

Figure 2: Plot of Magnetization versus Tube Diameter

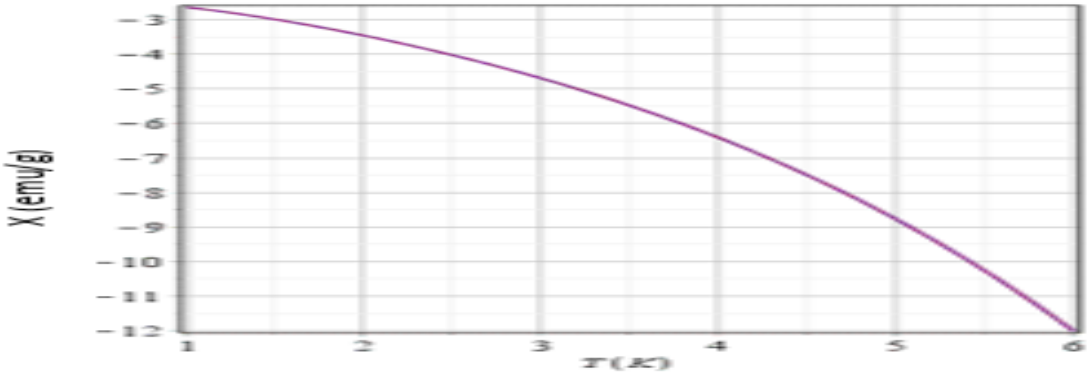

Figure 3: Plot of Susceptibility versus Temperatures

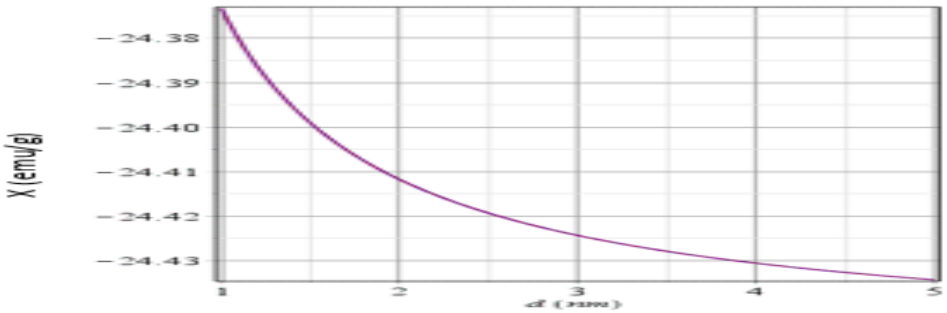

Figure 4: Plot of Susceptibility versus Tube's diameter

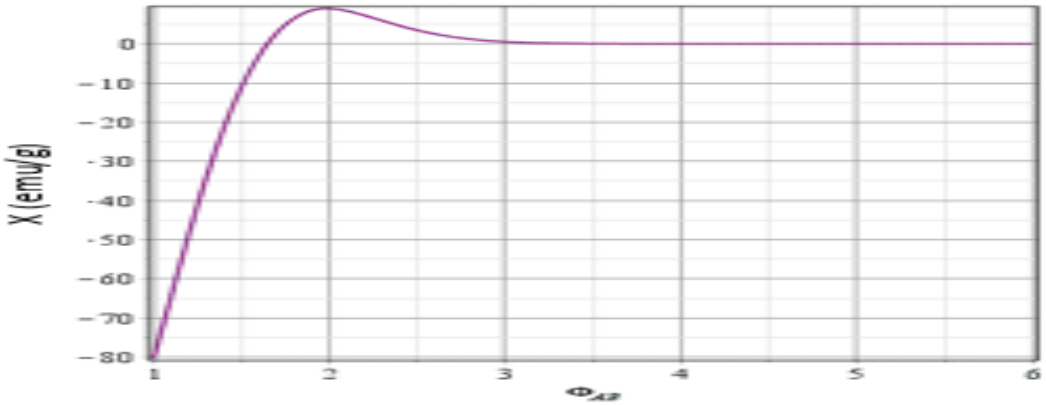

Figure 5: Plot of susceptibility versus AB flux.

4. Results And Discussion

Figure 1 depicts the plot of the magnetization against temperature. It is seen that the magnetization of the material decreases as the temperature is increasing. The increasing temperature brings about thermal disorder causing the atomic domains/spin in the material to become disordered, hence, the decrease in the magnetization. In figure 2, the plot of magnetization against the tube diameter of the carbon nanotube showed that the magnetization decreases in an exponential manner as the diameter increases. Here, the cylindrical nature of the tube necessitates the scaling of the orbital currents and quantization of the electronic states. The plot of magnetic susceptibility with temperature is shown in Figure 3. The magnetic susceptibility decreases as the temperature rises. An increase in the temperature causes the disruption of the delocalized π-electron framework thus decreasing the magnetic susceptibility (Ibwanga, 2021). Again, CNT as diamagnetic material depicts a negative magnetic susceptibility (Charles, 2005). Figure 4 shows the plot of magnetic susceptibility as a function of the tube's diameter. It is noticed that the magnetic susceptibility decreases exponentially with the tube diameter due to the net scaling of the orbital magnetic moments and density of states which makes the susceptibility scaling inversely with the diameter. Therefore the more the tube diameter becomes larger, the diamagnetism

per volume becomes lesser. The plot of susceptibility versus Aharonov-Bohm (AB) flux is shown in figure 5. CNT being a diamagnetic material, has the electron spin of the atoms or molecules paired, hence, their magnetic moment is zero. So on the application of external magnetic field, the phenomenon of Lenz's law will cause the induce current to oppose the flux change thereby leading to negative magnetic susceptibility.

5. Conclusion

The magnetic properties of zig-zag single-walled (8,0) carbon nanotube has been investigated in the presence of magnetic field and Aharonov-Bohm (AB) flux using the NU method. The partition function calculated with the energy eigen value equation was used to evaluate the magnetic properties of the carbon nanotube. The results of the graphical analysis of the plot of magnetization as a function of temperature and tube's diameter revealed that the magnetization of the carbon nanotube decreases with increasing temperature and tube's diameter. The magnetic susceptibility also decreases as the temperature and tube's diameter were increasing. The plot of susceptibility against Aharonov-Bohm flux showed that the carbon nanotube has a negative magnetic susceptibility. Thus, the zig-zag single-walled (8,0) carbon nanotube exhibited a diamagnetic feature.

Statements And Declaration

Funding Statement

The author did not receive any funding from any organization.

Conflict Of Interest

The author declare no conflict.

References

Abbasi, I., 2024.Are Carbon Nanotubes Magnetic? AZoNano. https://www.azonano.com/article.aspx? Article ID=6748.

Ando, T., 2005.Theory of Electronic States and Transport in Carbon nanotubes. *Journal of the Physical Society of Japan,* 74 (3) Pp. 777-817.

Angelsky, O., Ivashko, V., and Maksimyak, P., 2020.Magnetic Properties of Single-Walled Carbon nanotube with Mixed Spins: Monte Carlo Study. Low Dimensional Materials and Devices. 2020 doi:10. 1117/12.2567606.

Atkins, P., and De Paula, J., 2009. Statistical thermodynamics 2: application. Physical Chemistry, 8th Edition, Chapter 17. Oxford University Press. Scientific Research Publishing.

Avouris, P., Appenzeller, J., Martel, R., and Wind, S., 2003. Carbon Nanotube Electronics. Proceedings of the IEEE, Vol 91 No. 11.

Boyacioglu, B., and Chatterjee, A., 2012. Dia and Paramagnetism and total susceptibility of GaAs quantum dots with Gaussian confinement. *Physica E* 44, 1826-1831.

Cano, M. E., Cordova-Fraga, T., Sosa, M., Bernal-Alvarado, J., and Baffa, O., 2008.Understanding the Magnetic Susceptibility Measurements by using Analytical Scale. *Eur. J. Phys*. 29 Pp. 345-354 doi:10.1088/0143-0807/29/2/015

Cornell, M. J. O., 2006. Carbon Nanotubes. Properties and Applications. CRS press, Inc.,.

Dass, D., and Vaid, R., 2017. Chirality dependence of electronic band structure and density of states in single-walled carbon nanotubes. *The African Review of Physics* 12: 0015

Dass, D., Prasher, R., and Vaid, R., 2012).Analytical Study of Unit Cell and Molecular Structures of Single Walled Carbon Nanotubes. *International Journal of Computational Engineering Research* Vol. 2 Issue 5, 2012.

Dresselhaus, M. S., Dresselhaus, G., and Jorio, A., 2008. Carbon Nanotubes: Advanced Topics in the Synthesis, Structure, Properties and Applications. Springer-Verlag Berlin Heidelberg.

Eshghi, M., & Mehraban, H., 2017. Study of a 2D charged particle confined by a magnetic and AB flux fields under the radial scalar power potential. Eur. Phys. J. Plus 132:121 doi: 10.1140/epjp/i2017-11379-x

Folaron, D. R., 2021.Manipulating of Carbon Nanotube Growth Direction Utilizing Magnetic fields. Studying the Effect of Novel growth Mechanisms on Carbon Nanotubes. A Thesis Submitted for the Degrees of Master of Science in Materials Science and Engineering and Bachellor in Physics. Rochester Institute of Technology.

Ibwanga, S., Sodisetti, V. R., Coleman, C., Ncube, S., de Sousa, A. S., Erasmus, R. M., Flahaut, E., Blon, T., Lassagne, B., Samoîil, T., and Bhattacharyya, S., 2021. Tuning magnetic Properties of a Carbon Nanotube-Lanthanide Hybrid Molecular Complex through Controlled Functionalization. Molecule 2021, 26, 563. https://doi.org/ 10.3390/ molecules 26030563

Ikot Akpan, N., Chukwuocha, E. O., Onyeaju, M. C., Onate, C. A., Ita, B. I., andUdoh, M. E., 2018. Thermodynamic properties of diatomic molecules with general molecular potential. Pramana – Journal of Physics, 90, 23. https://doi.org/10.1007/s12043-017-1510-0

Khordad, R., and Rastegar Sedehi, H. R., 2017.Thermodynamic Properties of a Double Ring-Shaped Quantum at Low and High Temperatures. *J. low Temp. Phys.* DOI: 10.1007/s10909-017-1831-x.

Kim, I. T., Tannenbaum, A., and Tannenbaum, R., 2011. Magnetic Carbon Nanotubes: Synthesis, Characterization, and Anisotropic Electrical Properties, Electronic Properties of Carbon Nanotubes, Prof. Jose Mauricio Marulanda (Ed), ISBN: 978-953-307-499-3,.

Kittel, C., 2005.Introduction to Solid State Physics. Chapter 11 page 299. Eight Edition 2005. John and Sons Inc.

Lu, J. P., 1995. Novel magnetic Properties of Carbon nanotubes. *Physical Review Letter*, 74 (7) 1123-1126.

Moghaddam, H. K., Maraki, M. R., and Rajaei, A., 2020.Application of Carbon nanotubes (CNT) on the computer science and electrical engineering: a review. International Journal of Reconfigurable and Embedded Systems *(IJRES)* Vol. 9. No. 1, Pp.61-82.

Nanot, S., Thompson, N. A., Kim, J.-H., Wang, X., Rice, W. D., Pint, C. L., and Kono, J., 2013. Single-Walled Carbon Nanotubes. Springer Handbook of Nanomaterials, DOI: 10.1007/978-3-642-20595-8_4, Springer-Verlag Berlin Heidelberg.

Otete, I., and Eleje, C. B., 2023. Asian Research Journal of Current Science. Vol 5, Issue 1, Pp 20-27,.

Otete, I., Enaroseha, O. E., Okunzuwa, S. I., and Ejere, A. I. I., 2024. Spectra and Thermodynamic Properties Zig-Zag Single-Walled Carbon Nanotubes with Deng-Fan-Hulthen Potential. Ukr. J. Phys. 69 No.10, 719. https://doi.org/10.15407/ujpe69.10.719.

Ovchinnikov, A. A., and Atrazhov, V., 1998.Magnetic susceptibility of multilayered carbon nanotubes. *Physics of the* Solid State Vol. 40 No. 10.

Saifuddin, N., Raziah, A. Z., and Junizah, A. R., 2013.Carbon Nanotubes: A Review on structure and their Interaction with Protein Journal of Chemistry http://dx.doi.org/10.1155/2013/676815.

Samadishadlou, M., Farshbat, M., Annabi, N., Kavetskyy, T., Khalilov, R., Saghfi, S., Akbarzadeh, A., and Mousavi, S., 2017.Magnetic carbon nanotubes preparation, physical properties, and applications in biomedine, Artificial Cells, Nanomedicine and biotechnology. DOI: 10.1080/2191401. 2017.1389746.

Searles, T. A., Imanaka, Y., Takamasu, T., Ajiki, H., Fagan, J. A., Hubbie, E. K., and Kono, J., 2010.Large Anisotropy in the Magnetic Susceptibility of Metallic Carbon Nanotubes. Physical Review Letters 105, 017403 2010. DOI: 10.1103/Phys. Rev. Lett. 105.017403. 4950.

Sun, C., and Pokrovsky, V. L., 2024. Judul. Magnetic Properties of Nanotubes. DOI:10.5772/intechopen.115549.

Sun, K. J., Wincheski, R. A., and Park, C., 2008. Magnetic Property Measurements on Single Wall Carbon nanotube-polyimide composites. Journal of Applied Physics. 103, 023908 http://doi.org/10.1063/1.2832616

Tien, C. L., and Lienhard, J. H., 1985.Statistical Thermodynamics Chapter 3 and 5. Hemsphere Publishing Corporation. Washington, New

Tong, D., 2012. Statistical Physics, University of Cambridge Path 2. Mathematical Tripos. http://www.damp.com.ac.uk/user/tong/statphys.html.

Tsai, C. C., Chen, S. C., Shyu, F. L., Chang, C. P., and Lin, M. F., 2005.Magnetization of Carbon nanotubes. Physica E 30 (2005) Pp. 86-92 doi:10.1016/ j.physe.2005.07.003

Wong, P. H. S., and Akinwande, D., 2011.Carbon Nanotube and Graphene Device Physics.

Zeinalipour-Yazdi, C. O., Loizidou, E. Z., and Chutia, A., 2019. Size-dependent bond dissociation on enthalpies in single-walled carbon nanotubes. *Chemical Physics Letters* 731 136628.

Zhou, C.-C., and Dai, W.-S., 2018. Calculating eigenvalues of many-body systems from partition functions.